Sparse Representation of Group-Wise FMRI Signals

Jinglei Lv[1,2], Xiang Li[2], Dajiang Zhu[2], Xi Jiang[2], Xin Zhang[1,2], Xintao Hu[1], Tuo Zhang[1,2], Lei Guo[1,2], and Tianming Liu[2]

[1] School of Automation, Northwestern Polytechnical University, Xi'an, China,
[2] Department of Computer Science and Bioimaging Research Center,
The University of Georgia, Athens, GA, USA

Abstract. The human brain function involves complex processes with population codes of neuronal activities. Neuroscience research has demonstrated that when representing neuronal activities, sparsity is an important characterizing property. Inspired by this finding, significant amount of efforts from the scientific communities have been recently devoted to sparse representations of signals and patterns, and promising achievements have been made. However, sparse representation of fMRI signals, particularly at the population level of a group of different brains, has been rarely explored yet. In this paper, we present a novel group-wise sparse representation of task-based fMRI signals from multiple subjects via dictionary learning methods. Specifically, we extract and pool task-based fMRI signals for a set of cortical landmarks, each of which possesses intrinsic anatomical correspondence, from a group of subjects. Then an effective online dictionary learning algorithm is employed to learn an over-complete dictionary from the pooled population of fMRI signals based on optimally determined dictionary size. Our experiments have identified meaningful Atoms of Interests (AOI) in the learned dictionary, which correspond to consistent and meaningful functional responses of the brain to external stimulus. Our work demonstrated that sparse representation of group-wise fMRI signals is naturally suitable and effective in recovering population codes of neuronal signals conveyed in fMRI data.

Keywords: DTI, Task-based fMRI, Sparse coding.

1 Introduction

The human brain function intrinsically involves complex processes with population codes of neuronal activities [1-2, 4]. In the neuroscience community, a large amount of research has supported that when determining neuronal activity, sparse population coding is an effective exploration [3]. For example, the primary visual cortex V1 receives image signals with a sparse set of sensory neurons [2], and similarly, the middle temporal lobe (MTL) neurons fire selectively to visual stimulus [4]. In other words, a sparse set of neurons encode specific concepts rather than responding to the input independently [3]. Inspired by these findings, significant amount of research efforts from the machine learning and pattern recognition fields has been recently devoted to sparse representations of signals and patterns, and remarkable achievements have been made [5].

K. Mori et al. (Eds.): MICCAI 2013, Part III, LNCS 8151, pp. 608–616, 2013.

In general, fMRI neuroimaging takes the advantage of the coupling between neuronal activities and hemodynamics in the human brain, and thus fMRI signals, in principle, represent the population codes of large-scale neuronal activities. Given the remarkable successes of sparse representations in the machine learning and pattern recognition fields [5], in which the achievements were originally inspired and motivated by brain sciences discoveries, it is natural and well-justified to explore sparse representation of fMRI signals and the associated brain activity patterns. In the literature, there have been several pioneering efforts along this direction. For instance, a data-driven sparse coding fMRI analysis approach with K-SVD method and general linear model were developed to extract more accurate individually adaptive activation patterns in [6]. In [7], the authors used the Fisher Discriminative Dictionary learning (FDDL) method to cluster and differentiate functional brain states in resting and under task performance based on resting state fMRI and task-based fMRI datasets [7]. However, there have been very few studies that aim to examine the sparse representation of fMRI signals at the population level and to investigate how atoms in the learned sparse dictionary correspond to meaningful functional brain responses.

To address the above questions, in this paper, we design and apply a novel group-wise sparse representation framework for task-based fMRI signals from multiple subjects via dictionary learning methods. Specifically, we employ an effective online dictionary learning method [8] to learn an over-complete dictionary for group-wise sparse representation of the fMRI signals pooled from large-scale corresponding cortical landmarks of a group of subjects. For each subject, we adopted the publicly available DICCCOL (Dense Individualized and Common Connectivity-Based Cortical Landmarks) system [9] to locate 358 consistent cortical landmarks based on DTI data. Since the 358 DICCCOLs have been shown to possess intrinsic structural and functional correspondence across subjects [9], we extract fMRI signals for each of them across a group of subjects and then the pooled fMRI signals are used to learn a dictionary for group-wise sparse representations based on optimally determined dictionary size. The major advantage of using DICCCOL is that the small set of samples reduce the computing consume for group analysis, and the anatomical correspondence enable statistical exploration to the spare representation. Applications of this novel framework on a working memory task-based fMRI dataset [10] have identified meaningful Atoms of Interests (AOI) in the learned dictionary, corresponding to consistent and meaningful functional responses of the brain to block-based external stimulus.

2 Materials and Methods

2.1 Overview

Our novel computational framework of group-wise sparse representation of fMRI signals is summarized in Fig.1. First, 358 corresponding DICCCOL landmarks (Fig.1a) are localized and optimized on DTI datasets of all subjects via the methods in [9]. For each subject, after the linear intra-subject image registration of DTI and fMRI data, we extract task-based fMRI signal for each landmark. Then, the signals of 358

landmarks from k subjects are arranged into a signal matrix $S \epsilon \mathbb{R}^{t \times n}$ (Fig.1b) in order, where n columns are representative fMRI signals from the landmarks of k subjects ($n_1 = n_2 = \ldots = n_k = 358$, $n = n_1 + n_2 + \ldots + n_k = k \times 358$), and t is the fMRI volume number. By using an effective online dictionary learning and sparse coding method [8], each fMRI signal vector in S will be modeled as the linear combination of atoms of a learned dictionary D (Fig.1c), i.e. $s_i = D \times \alpha_i$ and $S = D \times \alpha$, where α is the coefficient matrix for sparse representation and each column α_i is the corresponding coefficient vector for s_i. Finally, as shown in Fig.1d, we optimize the dictionary size, identify meaningful Atoms of Interests (AOI), and perform statistics and interpretations on the sparse α matrix in the context of the correspondences of DICCCOL landmarks.

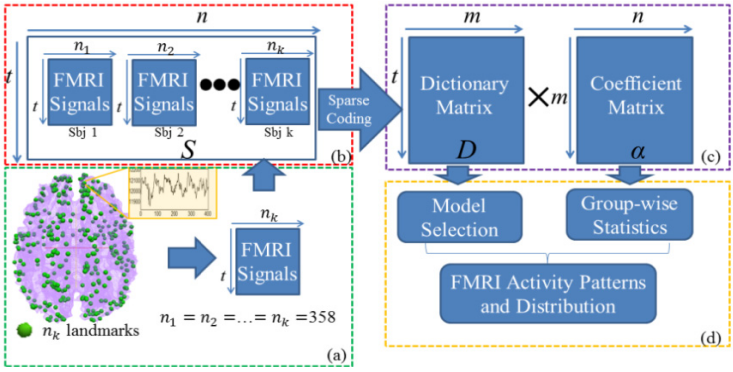

Fig. 1. The framework of sparse representation of group-wise fMRI signals

2.2 Data Acquisition and Pre-processing

In an IRB approved working memory task-based fMRI experiment [10], fMRI images of 19 subjects were scanned on a 3T GE Signa scanner. Briefly, acquisition parameters are as follows: fMRI: 64×64 matrix, 4mm slice thickness, 220mm FOV, 30 slices, TR=1.5s, TE=25ms, ASSET=2. Each participant performed a modified version of the OSPAN task (3 block types: OSPAN, Arithmetic, and Baseline) while fMRI data is acquired. DTI data was acquired with dimensionality 128×128×60, spatial resolution 2mm×2mm×2mm; parameters are TR 15.5s and TE 89.5ms, with 30 DWI gradient directions and 3 B0 volumes acquired. Detailed task design and preprocessing steps are referred to [10]. For each subject, the 358 DICCCOL landmarks are localized and optimized via the computational framework in [9]. DTI images of each subject were registered into the fMRI space via FSL FLIRT. As landmarks were localized and optimized on the white matter cortical surfaces of DTI data, we first translate the landmark locations into voxels of DTI image, and with the registration of DTI and fMRI data, we then locate the landmarks on fMRI images and extract corresponding fMRI signal for each landmark. As our work majorly focused on the fluctuation of fMRI signals, we normalize each extracted signal to have *zero* mean and standard deviation of 1.

2.3 Dictionary Learning

In our approach, we aim to learn a meaningful and over-complete dictionary $D \epsilon \mathbb{R}^{t \times m}$ (m>t, m<<n) [8] for the sparse representation of S. For the signal set $S = [s_1, s_2, \dots s_n] \epsilon \mathbb{R}^{t \times n}$, the empirical cost function is summarized as Eq.(1) considering the average loss of regression to n signals.

$$f_n(D) \triangleq \frac{1}{n} \sum_{i=1}^{n} \ell(s_i, D), \tag{1}$$

With the aim of sparse representation using D, the loss function is defined in Eq.(2) with a ℓ_1 regularization that yields to a sparse resolution of α_i, and here λ is a regularization parameter to trade off the regression residual and sparsity level.

$$\ell(s_i, D) \triangleq \min_{\alpha_i \epsilon \mathbb{R}^m} \frac{1}{2} ||s_i - D\alpha_i||_2^2 + \lambda ||\alpha_i||_1 \tag{2}$$

As we majorly focus on the fluctuation shape of basis fMRI activity and also in order to prevent D from arbitrarily large values, columns $d_1, d_2, \dots \dots d_m$ are constrained with Eq.(3).

$$C \triangleq \left\{ D \epsilon \mathbb{R}^{t \times m} \quad s.t. \quad j = 1, \dots m, \qquad d_j^T d_j \leq 1 \right\} \tag{3}$$

$$\min_{D \epsilon C, \alpha \epsilon \mathbb{R}^{m \times n}} \frac{1}{2} ||S - D\alpha||_F^2 + \lambda ||\alpha||_{1,1} \tag{4}$$

In summary, the whole problem can be rewritten as a matrix factorization problem in Eq.(4) [8], and we use the effective online dictionary learning method in [8] to learn the dictionary for sparse representation of group-wise fMRI signals on corresponding DICCCOL landmarks.

2.4 Sparse Representation and Group-Wise Analysis

With sparse representation, the most relevant bases of fMRI activity are selected and linearly combined to represent the original fMRI signals. The Orthogonal Matching Pursuit algorithm [11] is employed to represent a given signal using the dictionary learned D with the ℓ_0 regularization $||\alpha_i||_0 \leq L$ [11], as present in Eq.(5), where L is the largest number of atoms in D that are allowed to use in regression .

$$\min_{\alpha_i \epsilon \mathbb{R}^m} ||s_i - D\alpha_i||_2^2 \ , \ s.t. \ ||\alpha_i||_0 \leq L \tag{5}$$

Afterwards, for each signal in S, we obtain a corresponding coefficient vector which is a column of α in Fig.1 and Fig.2. The matrix of α is decomposed into k sub-matrices for DICCCOL landmarks of each subject, as illustrated in Fig.2. The element (i,j) in each sub-matrix stores the weight coefficient to the i^{th} atom in the dictionary of the j^{th} DICCCOL landmark (Fig.2). With a group-wise null hypothesis t-test, we determine the non-zero reference (i,j) as a group-wise effective landmark reference to the i^{th} atom of the j^{th} landmark. Then, with the statistics of global reference rates and

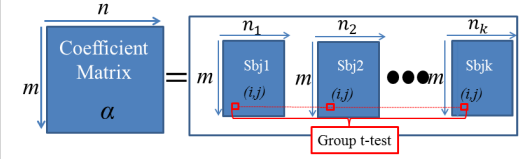

Fig. 2. Decomposition of the α matrix to k subjects, and group-wise null hypothesis t-test for each weight

group-wise effective landmark reference rate, we select the most popular dictionary atoms and map them to the DICCCOL landmark atlases for further analysis.

In our proposed pipeline, we train dictionary with a weak l_1-*norm* (λ in Eq.(4) is set with a small value) in order to minimize the representation residual and guarantee the atom signals' quality in D. While in the representation step, we choose a strong l_0-*norm* (L in Eq.(5) is set with a small integer) with the purpose of discriminating ROIs using the same smallest number of explanatory atoms from the learned D. In this way, we trade off the reliability of D and discriminative capability of α.

3 Experimental Results

3.1 Dictionary Size Selection

With the online dictionary learning method [8], we learned the dictionary for sparse representation of our signal dataset. Here, the parameter λ is set with a small value of 0.15 in order to learn dictionary with relatively less representation residual [8]. Note that we tried different settings of λ from 0.5-2.0 with a fixed dictionary size, and the learned dictionaries are quite similar in term of corresponding atom signals' shape. There are no common criteria to determine the size of learned dictionary for the online dictionary learning method. But a good dictionary should be efficient while being not overfitting [8]. In term of efficiency, the representation residual should be minimized, and meanwhile the atoms should be less correlated to avoid overfitting. As discussed in Section 2.3, the appropriate dictionary size m would be $m>t$, $m<<n$ (t=270, n=358×19=6802). Here, to select the optimal dictionary for our problem, we repeated the training with the m ranging from 300 to 900 with an interval of 50.

For each learned dictionary, we define the average representation residual as

$$R = \frac{1}{n}||S - DA||_F^2 \tag{6}$$

where A is the regression coefficient matrix of S using D , calculated with the method described in Section 2.4, and here we set the sparsity constraint $L=m$ to minimize R in each repeat. As plotted in Fig.3a, it is obvious that R is monotonically decreasing with larger dictionary size.

As the DICCCOL landmarks possess intrinsic structural and functional correspondence, we measure the consistency of representation for signals of each corresponding landmark. For each cortical landmark i, we collect the corresponding coefficient vectors from k subjects in A, as $a_i = [a_{i1}, a_{i2}, \ldots a_{ik}], a_{ij} \in \mathbb{R}^m$. And their consistency is measured by the Cronbach's α [12] as

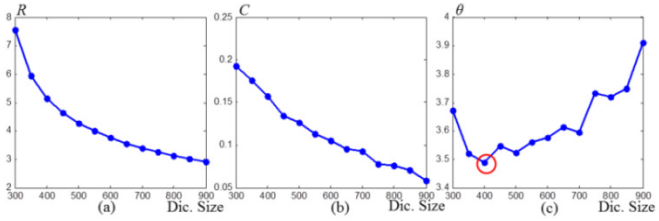

Fig. 3. The plotted values of R, C and θ with dictionary size vary from 300 to 900

$$c_i = \frac{k}{k-1}\left(1 - \frac{\sum_{j=1}^{k}\sigma_{a_{ij}}^2}{\sigma_{a_i}^2}\right) \tag{7}$$

The average consistency of all DICCCOL landmarks is:

$$C = \frac{1}{n_k}\sum_{i=1}^{n_k} c_i\,, (n_k = 358) \tag{8}$$

As shown in Fig.3b, *C* also decreases with increasing of the dictionary size.

In our approach, considering the correspondence of DICCCOL landmarks as a group-wise regularization, the *C* is supposed to be higher, while *R* is supposed to be lower. In order to trade-off the two criteria, we define

$$\theta = lnR - lnC \tag{9}$$

to select optimal dictionary size with the lowest θ value. In Fig.3c, we select the best dictionary size *m=400,* with the lowest θ value highlighted with a red circle.

3.2 Sparse Representation and Evaluation

We represented each fMRI signal in *S* with the sparsity constraint of *L*=20 using the method in Section 2.4. Statistics was performed on the global reference rate for each atom in the learned *D,* which was the signal number in *S* that refers to the atom, as shown in Fig.4a. We also performed statistics on the group-wise effective landmark reference rate in Section 2.4, which was the landmark number that possesses group-wise reference to each atom in Fig.4b. It is striking that in both Fig.4a and Fig.4b, we found 4 corresponding peaks that have both high global reference rate and group-wise landmark reference rate. These atoms are thus selected as Atoms of Interest (AOI). Notably, we tried different sparsity constraints of *L*=10, 20, 30 and 40, and it is interesting that the peaks AOIs are consistently the same, suggesting the robustness of

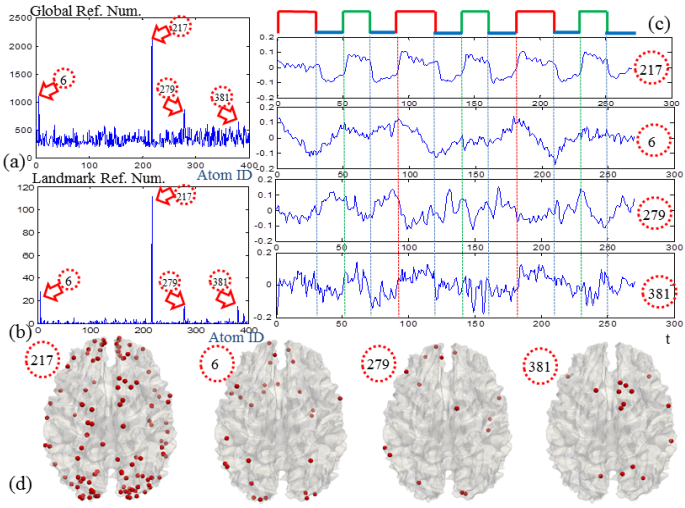

Fig. 4. (a) Global reference numbers of 400 atoms in the learned dictionary. (b) Group-wise landmark reference numbers of 400 atoms. (c) Atom shapes of 4 peaks in (a) and (b). (d) The landmark distributions with reference of the 4 AOIs respectively.

our methods. Also, the shapes of AOIs are compared with the task stimulus curve in Fig.4c. It is striking that all of the AOI shapes appear to be task-related response patterns. For instance, the AOIs #217 and #279 correspond to the task and anti-task responses; the AOI #6 exhibits half of the frequency of AOI #217; while AOI #381 shows similar global shape as AOI #217 but with much higher frequency fluctuations.

Afterwards, the DICCCOL landmarks that possess reference to each AOI in Fig. 4c are mapped to a cortical surface, respectively, in Fig.4d. These DICCCOLs were selected as landmarks of interest (LOI) that are involved in working memory task. Among all of the LOIs in Fig. 4d, the DICCCOLs, that possess reference to only one AOI, are visualized in Fig.5a, and the ones possessing references to multiple AOIs are shown in Fig.5b-5c. As a result, we separated the LOIs in Fig. 4d into 10 groups depending on the combinations of AOIs they refer to, with the number of each group shown in the 2nd row of Table 1 and spheres marked in Figs. 5a-5c with different colors. It is clear that the brain's responses to block task are complex, e.g., the landmarks in Fig.5a are only involved in one functional activity, but the landmarks in Fig.5b-5c are involved in multiple responses. These results not only support the importance of sparse representation of fMRI signals, but also demonstrate the multiple functional roles possibly played by the same cortical landmark.

For additional comparisons, we performed group-wise activation detection using the FSL FEAT based on the GLM and mixed-effect model [13] to the fMRI volumes of the same fMRI dataset. We mapped the detected activations (p-value=0.05, z-value>3.0) to the cortical surface as yellow regions in Figs. 5d-5f. The 10 groups of selected DICCCOLs in Figs. 5a-5c were overlaid on the activation maps of Figs. 5d-5f respectively for visual comparisons. It is evident that some DICCCOLs with the AOI #217 are within the activation maps, but many of them are outside of the activation maps, even though these landmarks possess a response component very similar to the stimulus curve. This result suggests that the red spheres referring to the AOI #217 might be a substantially more sensitive way to detect activated brain landmarks than the traditional FSL FEAT, considering different levels of noise.

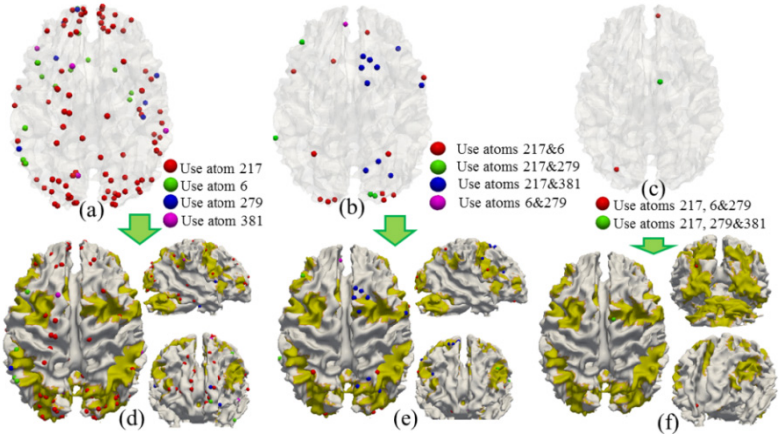

Fig. 5. (a) Landmarks with reference of only one of the 4 AOIs. (b) Landmarks with reference of two of the 4 AOIs. (c) Landmark with reference of three of the 4 AOIs. (d-f) are the activation maps detected by using group-wise activation detection (via FSL FEAT), overlaid with the landmarks in (a-c), respectively.

Table 1. The number of DICCCOLs of each group within the activation areas. The 2nd row is the total number of each DICCCOL group using different AOIs. The following four rows are the overlaid numbers with activations detected with different z-value thresholds.

Used AOIs	#217	#6	#279	#381	#217 &#6	#217 &#279	#217 &#381	#6 &#279	#217,#6 &#279	#217,#279 &#381
Total	83	13	7	4	12	4	10	1	2	1
z=2.5	37	1	3	2	9	3	6	0	1	1
z=3.0	33	1	2	2	9	3	6	0	1	1
z=3.5	23	1	1	2	7	3	5	0	1	0
z=4.0	14	0	1	1	6	3	5	0	1	0

For quantitative comparison, we selected activation foci with different z-value thresholds, and the DICCCOL numbers of the 10 groups that are within the yellow activation maps are presented in Table 1 (Rows 3-6). By comparing the total number of the 10 groups in the 2nd Row, we can see that even with a relatively low threshold (z-value=2.5), the traditional method by FSL FEAT can only detect a limited number of the selected DICCCOL landmarks that possess reference to AOI #217 with similar pattern as the stimulus curve. Also, it performs even poorer in detecting DICCCOLs that have other activity pattern (AOIs #6, #279 and #381). These results support that group-wise decoding of fMRI activity using sparse coding is much more robust to noise than GLM-based activation method, and is much more adaptive in decoding multiple task-related fMRI activity patterns.

4 Conclusion

We have described a novel group-wise sparse representation framework for task-based fMRI signals pooled via consistent DICCCOL landmarks, and demonstrated by extensive experiments that the framework can recover consistent and functionally meaningful atoms that represent population codes in task-based fMRI data. Our work demonstrated that sparse representation is effective in representing task-based fMRI signals and functional brain activity patterns. Thus, our work offers a promising general framework for representation and modeling of fMRI data.

References

1. Olshausen, B.A., Field, D.J.: Sparse coding of sensory inputs. Current Opinion in Neurobiology 14(4), 481–487 (2004)
2. Olshausen, B.A.: Emergence of simple-cell receptive field properties by learning a sparse code for natural images. Nature 381(6583), 607–609 (1996)
3. Daubechies, I., et al.: Independent component analysis for brain fMRI does not select for independence. Proceedings of the National Academy of Sciences 106(26), 10415–10422 (2009)

4. Quian Quiroga, R., Kreiman, G., Koch, C., Fried, I.: Sparse but not 'grandmother-cell'coding in the medial temporal lobe. Trends in Cognitive Sciences 12(3), 87–91 (2008)
5. Wright, J., et al.: Sparse representation for computer vision and pattern recognition. Proceedings of the IEEE 98(6), 1031–1044 (2010)
6. Lee, K., Tak, S., Ye, J.C.: A data-driven sparse GLM for fMRI analysis using sparse dictionary learning with MDL criterion. IEEE Transactions on Medical Imaging 30(5), 1076–1089 (2011)
7. Zhang, X., et al.: Characterization of Task-Free/Task-Performance Brain States. In: Ayache, N., Delingette, H., Golland, P., Mori, K. (eds.) MICCAI 2012, Part II. LNCS, vol. 7511, pp. 237–245. Springer, Heidelberg (2012)
8. Mairal, J., Bach, F., Ponce, J., Sapiro, G.: Online learning for matrix factorization and sparse coding. The Journal of Machine Learning Research 11, 19–60 (2010)
9. Zhu, D., et al.: DICCCOL: Dense Individualized and Common Connectivity-Based Cortical Landmarks. Cerebral cortex (2012), http://dicccol.cs.uga.edu/
10. Faraco, C.C., et al.: Complex span tasks and hippocampal recruitment during working memory. NeuroImage 55(2), 773–787 (2011)
11. Mallat, S.G., Zhang, Z.: Matching pursuits with time-frequency dictionaries. IEEE Transactions on Signal Processing 41(12), 3397–3415 (1993)
12. Cronbach, L.J.: Coefficient alpha and the internal structure of tests. Psychometrika 16(3), 297–334 (1951)
13. Beckmann, C.F., Jenkinson, M., Smith, S.M.: General multilevel linear modeling for group analysis in FMRI. Neuroimage 20(2), 1052–1063 (2003)